Original Paper

ADAMTS1 Promotes Adhesion to Extracellular Matrix Proteins and Predicts Prognosis in Early Stage Breast Cancer Patients

Izza A. Tan   Kate Frewin   Carmela Ricciardelli   Darryl L. Russell

Robinson Research Institute, Discipline of Obstetrics and Gynaecology, Adelaide Medical School, University of Adelaide, Adelaide, Australia

Abstract
Background/Aims: Despite, several studies demonstrating pro-metastatic effects of the metalloproteinase ADAMTS1 in breast cancer, its role in facilitating the metastatic cascade remains unclear. To date there have been limited studies that have examined the expression of ADAMTS1 in primary and metastatic breast cancer tissues. *Methods:* We assessed *ADAMTS1* mRNA levels in publically available breast cancer sets and analysed ADAMTS1 protein levels by immunohistochemistry in breast tissue microarrays containing normal breast tissue (n=9), primary invasive ductal breast carcinomas (n=79) and metastatic lesions (n=58). To understand the underlying events influenced by ADAMTS1 and provide a mechanism by which tumors expressing this protease promote metastasis, we assessed the ability of PyMT/*Adamts1+/+*, PyMT/*Adamts1+/-* and PyMT/*Adamts1-/-* primary mammary cancer cells to adhere to matrigel and migrate or invade towards a chemoattractive environment. *Results:* High *ADAMTS1* expression was associated with reduced disease-free survival, distant metastasis free-survival and overall survival in breast cancer patients with node negative disease. Although ADAMTS1 expression was reduced in primary breast cancers compared to normal tissue and not elevated in metastatic lesions, high ADAMTS1 immunostaining was associated with a higher number of positive lymph nodes (p=0.006) and the presence of distant metastasis (p=0.023). Depletion of *Adamts1* in mammary cancer cells impeded their adhesion to a biological matrix substratum and diminished cell migration but not invasion. *Conclusion:* The effects observed on cell adhesion and migration demonstrates a potential mechanism whereby ADAMTS1 promotes breast cancer metastasis.

© 2019 The Author(s). Published by
Cell Physiol Biochem Press GmbH&Co. KG

C. Ricciardelli and D. L. Russell contributed equally to this work.

Darryl L. Russell

Discipline of Obstetrics and Gynaecology, Adelaide Medical School, University of Adelaide
North Terrace, 5000, SA (Australia)
Tel. +61 08 8313 4096, E-Mail darryl.russell@adelaide.edu.au

Introduction

The most pernicious stage in cancer is metastasis. The metastatic process requires a series of complex events beginning with the escape of cancer cells from the primary tumor mass and subsequent dissemination into the vascular supply. In the circulation metastatic cells are capable of contact-independent survival. Next cancer cells extravasate from the vessel and establish residence in distant tissues to form secondary tumors. In order for the cascade of events involved in metastasis to occur, cancer cells require phases of increased adherence to the ECM and enhanced abilities to move within and invade through the ECM [1].

Matrix adhesion, migration and invasion are interdependent cell processes in cell physiology as well as in cancer. The ability of cancer cells to adhere to the surrounding environment is essential for the determination of front-rear cell polarity driving cancer cell migration [2-5], which is in turn necessary for cell invasion. Attachment of cells to the basement membrane is also required for the activity of proteolytic enzymes [6] that breakdown the structural constraints restricting cell movement and allowing cancer cells to traverse through its surrounding extracellular environment or penetrate the tissue boundary [6-8].

Cancer cells acquire essential molecular changes that promote the atypical remodelling of the peritumoral ECM environment, which ultimately permit metastatic disease progression. The upregulation of metalloproteases, enzymes dedicated to extracellular protein degradation, is a vital molecular event that accompanies and supports the transition to metastasis. Metalloproteases facilitate the significant remodelling of the peritumoral stroma by breaking down the structural components of the ECM and disintegrating the tissue framework that would otherwise inhibit cancer cell escape and restrict cell motility. In breast cancer, increased abundance of the metalloprotease ADAMTS1 strongly correlated with metastasis [9-16]. This had been demonstrated through comparative gene expression analysis between breast cancers with either no, weak or strong metastatic capacity [10, 11, 15] and in various experimentally-induced metastasis models (i.e. intravenous injection of breast cancer cells) [12, 13]. The pro-metastatic influence of ADAMTS1 was also depicted in an *in vivo* model of breast tumorigenesis whereby the loss of *Adamts1* significantly impeded the aggressive advancement and eventual metastasis of MMTV-PyMT breast tumors [9].

In this study we assessed the relationship of *ADAMTS1* mRNA expression with disease-free survival (DFS), distant-metastasis free-survival (DMFS) and overall survival (OS) in publically available breast cancer sets and analysed ADAMTS1 protein levels by immunohistochemistry in breast tissue microarrays containing normal breast tissue, primary invasive ductal breast carcinomas and metastatic lesions. We additionally assessed cell-matrix adhesion, motility and invasion of primary mammary cancer cells derived from PyMT/*Adamts1+/+*, PyMT/*Adamts1+/-* and PyMT/*Adamts1-/-* tumors.

Materials and Methods

Isolation and propagation of primary mammary cancer cells

Mammary tumors were resected from *Adamts1+/+*, *Adamts1+/-* and *Adamts1-/-* MMTV-PyMT transgenic mice at 16-20 weeks of age or when ethical euthanasia was necessary due to tumors reaching 3cm^3. Mammary tumors from all glands were weighed, collected and cut into 1mm^3 pieces, then incubated in dissociation buffer [2mg/ml collagenase A, 5U/ml hyaluronidase, 0.1%w/v deoxyribonuclease 1] (10mls) for 1h at 37°C with agitation. Cell suspension was filtered through a sterilised 40μm nylon net filter (Steriflip® Filter unit, Merck Millipore, Billerica, MA, USA) to separate undigested material from isolated primary mouse mammary cancer cells (1°mMCC). The cell suspension was spun at 1500rpm for 5mins, the supernatant layer was removed and the cell pellet was resuspended in 3ml of growth media [DMEM + 10% FBS + 1% PSF]. The 1°mMCC suspension (1ml) was then transferred into T75 flasks containing 10ml growth media and grown for approximately 3-4 days or until reaching 90% confluence. After reaching 90%

Cellular Physiology and Biochemistry

Cell Physiol Biochem 2019;52:1553-1568

DOI: 10.33594/000000108
Published online: 29 May 2019

© 2019 The Author(s). Published by
Cell Physiol Biochem Press GmbH&Co. KG

1555

Tan et al.: Adamts1 Promotes Adhesion to ECM

confluence, 1°mMCC were cryopreserved with 15% DMSO cryopreserving agent (Sigma-Aldrich Pty Ltd., Sydney, Australia). All primary cell lines were used at passage 2 in subsequent experiments. Briefly, cells were revived from liquid nitrogen into a T25 flask containing 5mls of growth media. After 48 h, primary cells were transferred into three T25 flasks and allowed to reach 70-80% confluence. This took approximately 48-72 h post-passage, after which cells were trypsinised and used in experiments described below. Growth media replacement was performed daily.

Immunocytochemistry

In order to quantify the percentage of mammary epithelial cancer cells comprising our isolated 1°mMCC culture, 5×10^3 primary cells were grown in 1 well of an 8-well chamber slide (Life Technologies Australia Pty Ltd, Mulgrave, Victoria, Australia) with 500μl growth media for 24 h in a 37°C humidified incubator. After 24h, media was removed and cells were fixed with -20°C methanol (1ml/well) (ChemSupply, Gillman, SA, Australia) for 10 mins followed by 1 min incubation in -20°C acetone (1ml/well) (Merck Millipore, Billerica, MA, USA). Each well was washed with PBS twice (1 ml/well) and incubated in 1ml PBS with 3%(v/v) H_2O_2 (Sigma-Aldrich Pty Ltd, Sydney, Australia) to inhibit endogenous peroxidase activity. Non-specific antibody binding was subsequently blocked with 5% rabbit serum (Sigma-Aldrich Pty Ltd, Sydney Australia) for 20 mins and incubated overnight at 4°C with 1:100 anti-cytokeratin endo-A primary antibody (DSHB, University of Iowa, USA), or negative controls incubated with 5% rabbit serum during the overnight incubation. Wells were then washed with 1ml PBS, incubated for 1 h with 1:400 rabbit anti-rat secondary antibody (Millipore Corporation, Billerica, MA, USA) and then with 1:500 Streptavidin (Sigma-Aldrich Pty Ltd, Sydney, Australia). Visualisation of positive staining was achieved after a 6 mins reaction with diaminobenzidene (Sigma-Aldrich Pty Ltd, Sydney, Australia). Slide were subsequently washed with Ethanol and Xylene solution and mounted using Pertex mounting medium (HD Scientific Supplies Pty Ltd, NSW, Australia). High-resolution images were captured using the Nanozoomer digital slide scanner. 10 images of each well were taken at 20x magnification using the NDP viewing software.

Positive and negative cells were quantified by counting and percentage of positive cells was calculated. Image analysis was performed blinded to the mouse genotypes.

Analysis of public databases

The Kaplan-Meier plotter tool (http:/kmplot.com/analysis/) was used to generate survival curves combining mean expression of probes *ADAMTS1* mRNA data (probes 222162_s-at & 222486_s_at) from public breast cancer datasets [17] Kaplan-Meier analysis was performed on the 2014 version database (n=4124) and patients were split by the best cut-off selected by the online plotter tool [17]. Disease-free survival (DFS), distant metastasis-free survival (DMFS) and overall survival (OS) data was available for 751, 324 and 107 breast cancer patients treated with systemic therapies including endocrine and chemotherapy, respectively. DFS, DMFS and OS data was available for 451, 162 and 77 lymph node negative breast cancer patients, respectively.

RNA isolation and qRT-PCR

Total RNA was isolated from the breast cancer cell lines (HS578T, MC-F, MB468, MDA-MB231 and MCF-10A, from ATCC) using Trizol (Invitrogen Australia Pty. Ltd.) as per manufacturers' instructions. RNA samples were then treated with DNase (Ambion Inc., Austin, TX, USA) and concentration of RNA was quantified using the Nanodrop (Delaware, USA) and stored in 10μl aliquots at -20°C. A total of 2.5μg of RNA in a 60μl reaction was reverse-transcribed using SuperScript™ III Reverse Transcriptase (Carlsbad, CA, USA) as per manufacturers' instructions. Human ADAMTS1 validated primers were purchased from Sigma-Aldrich. Primer optimisation and cDNA optimisation was performed with a range of concentrations and the optimal concentration was selected. The final reaction volume was 20 μL containing 2 μL aliquot of cDNA (10ng/μL) of each sample, 0.2 μL each of forward primer and reverse primers, 10 μL of SYBR Green and 7.6 μL of water. Real time PCR was performed in triplicates for each sample using the Rotor-Gene™ 6000 (Corbett Life Science, Sydney, Australia). Cycling parameters were: 50°C for 2 min, 95°C for 10 min and followed by 40 cycles of 95°C for 15 seconds and then 60°C for 60 seconds. The CT values expressed for all samples were normalised relative to the housekeeping gene L19. The mean CT values were obtained and the samples were calibrated level of MCF10a cell line using the $2^{-\Delta\Delta CT}$ quantitation method.

Cellular Physiology and Biochemistry

Cell Physiol Biochem 2019;52:1553-1568

DOI: 10.33594/000000108
Published online: 29 May 2019

© 2019 The Author(s). Published by
Cell Physiol Biochem Press GmbH&Co. KG

1556

Tan et al.: Adamts1 Promotes Adhesion to ECM

Western blotting

Protein samples were extracted from cancer cell lines and resuspended in RIPA buffer (25mM Tris HCl pH 7.6, 150mM NaCl, 1% NP-40, 1% sodium deoxycholate, 0.1% SDS. Cell extracts (8µg) were electrophoresised in 10% sodium dodecyl sulphate-polyacrylamide gels (SDS-PAGE) and transferred onto Hybond-C nitrocellulose membrane (Amersham), polyvinylidene fluoride (PVDF) overnight at 4°C. The membrane was blocked with 3% skim milk in Tris-buffered saline with containing 0.05% Tween-20 (TBS-T) for 1 hour. Membrane was then incubated with primary antibodies for 2 hours as follows: ADAMTS1, (C-terminal, Sigma, St. Louis, MS, USA) diluted 1:1000). For protein detection, anti-rabbit horseradish peroxidise-conjugated secondary antibody was used at 1:2000. Protein bands on membranes were visualised using enhanced chemiluminiescence (ECL, Amersham Biosciences, Little Chalfont, Buckinghamshire, England).

Immunohistochemistry

Breast tissue microarrays (TMA) composed of invasive ductal carcinomas (n=82), normal breast tissue (n=13) and lymph metastases (n=59) were purchased from Biomax.us (BR952, BR10010, T086). Slides were incubated on a heat plate at 60°C for 2 h and dewaxed in xylene and ethanol. The endogenous peroxidase activity of the sections was quenched with 0.3% H_2O_2 prior to microwave antigen retrieval with 0.1M citrate buffer at pH 6.0. Each tissue sample was blocked with 5% goat serum and incubated overnight at 4oC with rabbit polyclonal anti-ADAMTS1 (1:300, AB39194, Abcam). The secondary antibody used was a biotinylated goat anti- rabbit (1:400, Dako Australia) incubated for 1 h at room temperature followed by streptavidin-HRP (1:500, Dako, Australia). Immuno-reactivity was detected using diaminobenzidine/H_2O_2 substrate, counterstained with 10% haematoxylin (Sigma-Aldrich), dehydrated and mounted in Pertex. Normal ovarian tissue was used as a positive control and the negative control included the tissue sections without the primary antibody incubation step or with rabbit immunoglobulin instead of ADAMTS1 antibody. Slides were digitally scanned using the NanoZoomer (Hamamatsu Photonics, Hamamatsu, Japan) and ADAMTS1 immunostaining in cancer cells was independently scored by two observers using a visual scoring system; no staining, weak, moderate and strong, represented numerically as 0, 1+, 2+ and 3+ respectively.

Real time cell-based assay

Cell adhesion, migration and invasion analyses were performed with the xCelligence real-time cell analysis system (ACEA Biosciences, San Diego, CA, USA). Each assay was performed as per the manufacturer's protocol in triplicate/quadruplicate wells. For the adhesion assay, cells were seeded at $5x10^3$ cells/well in an E-plate coated with 5% v/v matrigel (BD Biosciences, North Ryde, NSW, Australia). Cells were allowed to adhere for 2 hr. Linear regression analyses of adhesion impedance between 0-2 hr were performed using GraphPad Prism® version 6 (GraphPad Software, La Jolla, California, USA). This analysis identified the slope of the line or the rate of cell adhesion to matrigel during the period of the assay. To measure migration and invasion, $2x10^4$ and $4x10^4$ cells/well, respectively were seeded in CIM-plates and allowed to migrate for 10 hr and invade for 40 hr. Due to an inherit low migration and invasion we previously characterised in MCF10A cells, migration and invasion assays were observed over 45h. Cells were seeded in serum-free media and allowed to traverse towards a 5% serum containing media across 8µm porous membranes non-coated (migration) or coated with a 5%v/v matrigel barrier (invasion). The rate of migration and invasion for each sample was identified by interpolating a sigmoidal curve over the migration/invasion profile using GraphPad Prism® version 6 (GraphPad Software, La Jolla, California, USA). The sigmoid regression model identifies the slope of the curve, which represents the rate during the period when cells were traversing, as well as an upper plateau phase where little or no further cell migration and invasion occurred allowed determination of the time taken to reach maximal cell migration/invasion.

Invasion and migration profiles were interpolated with a sigmoid regression curve using GraphPad Prism® version 6. Sigmoid analysis determined the slope of the logarithmic increase in cell index, which represented the rate at which cells progressively migrated/invaded through the microporous membrane. It also identified the point at which cell index plateaued and this defined the maximum cell index and the time taken for this to be reached.

Cellular Physiology and Biochemistry

Cell Physiol Biochem 2019;52:1553-1568

DOI: 10.33594/000000108
Published online: 29 May 2019

© 2019 The Author(s). Published by
Cell Physiol Biochem Press GmbH&Co. KG

1557

Tan et al.: Adamts1 Promotes Adhesion to ECM

Statistics

Statistical significance was determined by One-Way ANOVA and Fisher's LSD *post hoc* test in GraphPad Prism® version 6 (GraphPad Software, La Jolla, California, USA). For the ADAMTS1 immunostaining a Chi-Squared test or Signed rank test was used to assess relationship between tissue types and clinical and pathological parameters. Non-normally distributed data were logtransformed prior to statistical analysis. Statistical significance was defined at $p \leq 0.05$.

Results

ADAMTS1 expression in breast cancer

ADAMTS1 expression was assessed by immunohistochemistry in normal breast (n=9), primary breast cancer (n=79) and metastatic lesions (n=58). Human ovary tissue was used as a positive control and consistent with previous studies, high ADAMTS1 immunoreactivity was observed in the granulosa cells of large ovarian follicles (Fig. 1a) [18]. ADAMTS1 was localized primarily to the ductal glands in the normal breast tissues. High ADAMTS1 immunostaining (score 2 or 3) was present in 88.9% (8/9) of the normal breast tissues examined (Fig. 1b). Variable ADAMTS1 immunostaining was observed in the cancer tissues. Up to 64.6% (51/79) of the primary breast cancers and 48% (28/58) of the metastatic tissues had high ADAMTS1 immunostaining (Table 1, a). Examples of primary breast cancers with low and high ADAMTS1 immunostaining are shown in Fig. 1c and Fig. 1d, respectively. A significantly higher proportion of normal breast tissues had high ADAMTS1 immunostaining compared to the primary and metastatic cancers (Table 1, a; p = 0.034). Pair analysis on matching primary and lymph node metastases (n=52) was also performed and showed no significant difference in ADAMTS1 immunostaining, p=0.083, Wilcoxon Signed rank test, Fig. 1e and Fig. 1f). No relationship was observed between ADAMTS1 immunostaining and breast cancer clinical stage, (p = 0.633, Table 1, b) or tumor grade (p = 0.064, Table 1, c), however, high ADAMTS1 immunostaining in the primary cancers was associated with a higher number of positive lymph nodes (Table 1, d; p=0.006) and the presence of
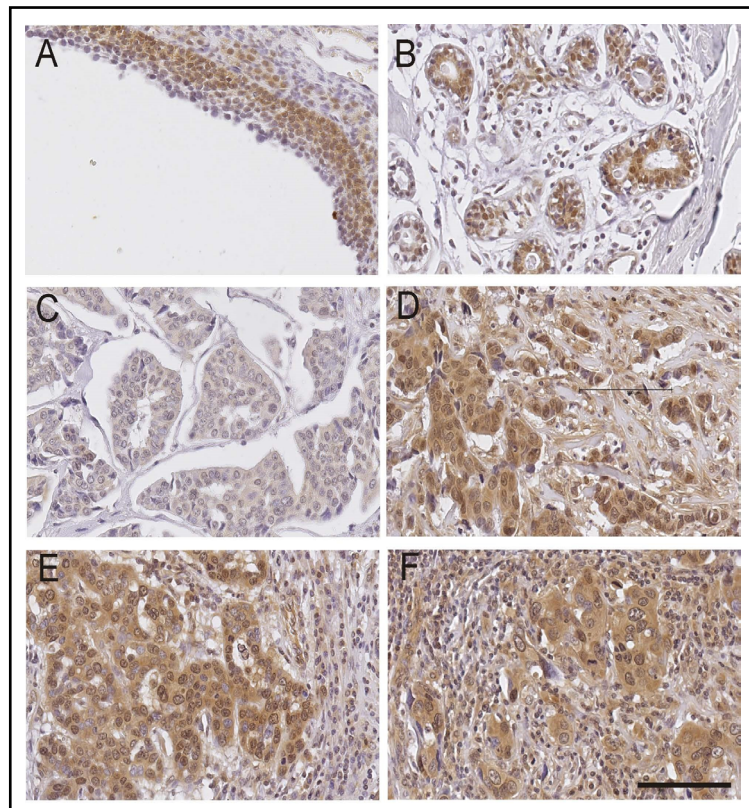

Fig. 1. ADAMTS1 immunohistochemistry. a) normal ovary, b) normal breast tissue, c) breast cancer tissue with low ADAMTS1 immunostaining, d) breast cancer tissue with high ADAMTS1 immunostaining. e) and f) are matching primary and metastatic breast cancer tissues from the same patient. scale bar = 100µm, all images are the same magnification.

Cellular Physiology and Biochemistry

Cell Physiol Biochem 2019;52:1553-1568

DOI: 10.33594/000000108
Published online: 29 May 2019

© 2019 The Author(s). Published by
Cell Physiol Biochem Press GmbH&Co. KG

1558

Tan et al.: Adamts1 Promotes Adhesion to ECM

distant metastasis (Table 1, e; *p* = 0.023). We also confirmed high expression of *ADAMTS1* mRNA and protein in metastatic breast cancer cell lines, Hs578T and MDA-MB231 and low expression in MB468, MCF-7 and MCF-10A cells (Supplementary Fig. 1 - for all supplemental material see www.cellphysiolbiochem.com). Consistent with these findings we found that high ADAMTS1 mRNA expression was significantly associated with reduced DMFS (Fig. 2c, *p*=0.003) and OS (Fig. 2e, p=0.023) in breast cancer patients receiving systemic treatments but not DFS (Fig. 2a). In patients with lymph node negative disease, high ADAMTS1 expression was significantly associated with reduced DFS (Fig. 2b, *p*=0.02), DMFS (Fig. 2d, *p*=0.0012) and OS (Fig 2f, *p*=0.014).

Table 1. Summary data of ADAMTS1 immunostaining and relationship with clinical and pathological characteristics. Statistical analysis was performed using Chi-Square test

Characteristics		ADAMTS1	
a. Tissue Type	Low (0 or 1)		High (2 or 3)
Normal breast	1/9 (11.1%)		8/9 (88.9%)
Primary breast cancer	28/79 (35.4%)		51/79 (64.5%)
Metastatic breast cancer	30/58 (52.0%)		28/58 (48.0%)
p-value		0.029*	
b. Breast cancer stage	Low (0 or 1)		High (2 or 3)
Stage 2	19/50 (38.0%)		31/50 (62%)
Stage 3	9/28 (32.1%)		19/28 (67.9%)
p-value		0.633	
c. Tumor grade	Low (0 or 1)		High (2 or 3)
1	3/8 (37.5%)		5/8 (62.5%)
2	22/51 (43.1%)		29/51 (56.9%)
3	2/17 (11.8%)		15/17 (88.2%)
p-value		0.064	
d. Lymph node status	Low (0 or 1)		High (2 or 3)
Negative	1/11 (9.4%)		10/11 (90.9%)
1-4	18/42 (42.9%)		24/42 (57.1%)
5 or more	0 (0%)		11/11 (100%)
p-value		0.006	
e. Distant Metastasis	Low (0 or 1)		High (2 or 3)
No	28/69 (40.6.2%)		41/69 (59.4%)
Yes	0/9 (0%)		9/9 (100%)
p-value		0.023	

PyMT/Adamts1-/- primary cells exhibited reduced adhesion to matrigel compared with Adamts1+/+ and Adamts1+/- primary mouse mammary cancer cells

Consistent with our previous report [9], total tumor mass as a proportion of body weight was significantly lower in PyMT/Adamts1-/- (6.88% ± 0.77) mice than in PyMT/Adamts1+/- (12.94% ± 1.31) and PyMT/Adamts1+/+ (10.66% ± 1.55) littermates (*p*=0.0019, One-way ANOVA; Fig. 3a). As there are heterogeneous cell populations that comprise mammary tumors, it was essential to determine the percentage of mammary epithelial cancer cells present in the cell isolates. To quantify the proportion of mammary epithelial cancer cells, immunocytochemistry was performed against the epithelial cell marker, cytokeratin endo-A, an endodermal cytokeratin expressed by mammary cancer cells) [19] (Fig. 3b-g). The isolated mammary tumors cells contained predominantly epithelial derived cells, the percentage of positive cells did not differ between PyMT/*Adamts1+/+* (61.76% ± 13.45), *Adamts1+/-* (61.70% ± 6.30) and *Adamts1-/-* (74.66% ± 4.41) 1°mMCC (Fig. 3h). The, cytokeratin negative cells are likely to be stromal fibroblasts and endothelial cells.

Adhesion of MCF10A mammary epithelial cell line, PyMT/*Adamts1+/+*, PyMT/*Adamts1+/-* and PyMT/*Adamts1-/-* primary cells to matrigel over a 2 h period was assessed using the xCELLigence real-time cell analysis system (Fig. 4a). MCF10A, a non-tumor human breast epithelial cell line was used as a homogeneous inter-assay experimental control and results from these indicated the small variability between replicate experiments, but also importantly showed markedly lower matrigel adhesion in the MCF10A breast epithelial cell line than 1°mMCC. Adherence of 1°mMCC derived from PyMT/*Adamts1+/+*, PyMT/*Adamts1+/-* and PyMT/*Adamts1-/-* to the matrigel substratum increased progressively throughout the 2 h time period (Fig 4a). When comparing the adhesion index of Adamts1+/+, Adamts1+/- and Adamts1-/- every 30 mins, no significant differences in adhesion were observed between the three Adamts1 genotypes 30 mins after the commencement of the assay. After 1 h in culture, *Adamts1-/-* cells adhesion index was significantly lower (0.088 ± 0.013) than *Adamts1+/+* (0.129 ± 0.006) and *Adamts1+/-* (0.140 ± 0.025) (*p*=0.015, One-way ANOVA; Fig. 4b). The differences in adhesion between *Adamts1* deficient and *Adamts1*
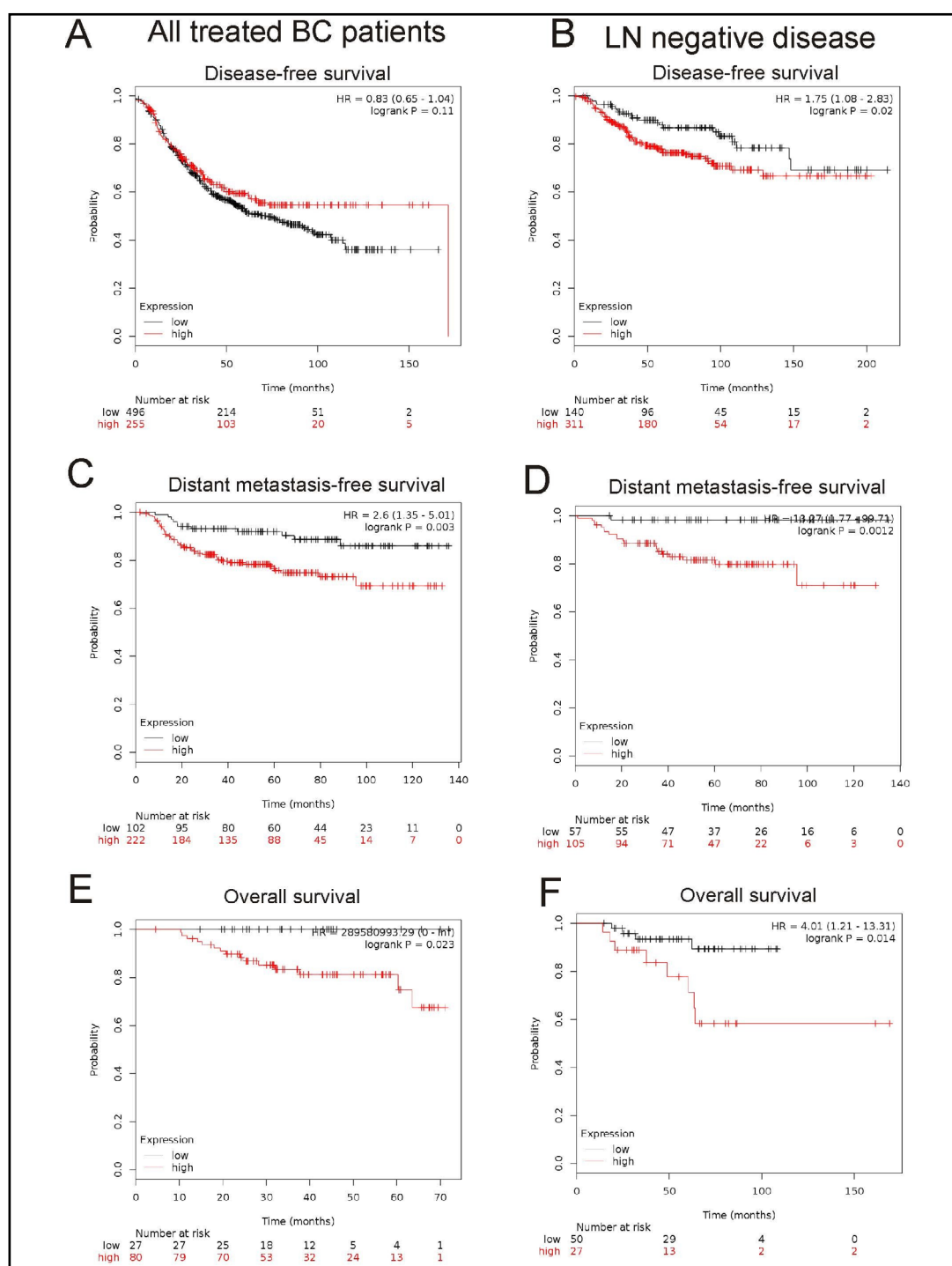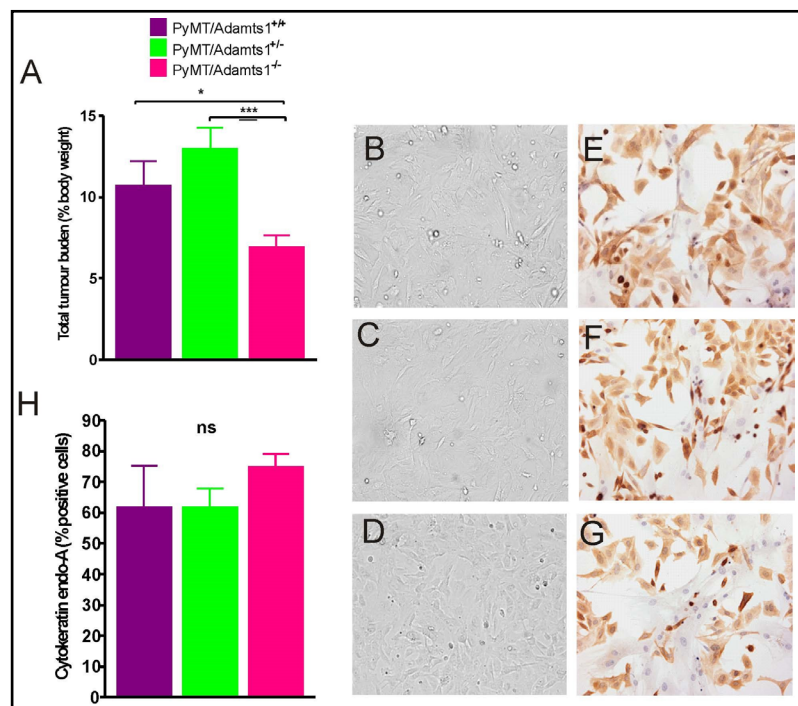
Fig. 2. Kaplan Meier survival analysis showing association of expression of ADAMTS1 with patient outcome. a) Disease-free survival curve in breast cancers patients that received systemic treatment with low or high levels of ADAMTS1 (mean Affymetrix probe set probes 222162_s-at & 222486_s_at, n=751). b) Disease-free survival curve in node negative breast cancers with low or high levels of ADAMTS1 (n=451). c) Distant metastasis-free survival curve breast cancers patients that received systemic treatment with low or high levels of ADAMTS1 (n=324). Distant metastasis free survival curve in lymph node breast cancers patients with low or high levels of ADAMTS1 (n=162). e) Overall survival curve in breast cancers patients that received systemic treatment with low or high levels of ADAMTS1 (n=107). f) Overall survival curve in lymph node positive breast cancers patients with low or high levels of ADAMTS1 (n=77).

Fig. 3. PyMT/*Adamts1-/-* mice have smaller mammary tumors than *Adamts1+/+* and *Adamts1+/-* littermates, and isolated 1°mMCC were predominantly of mammary epithelial cancer cell type. a) Mammary tumors were excised from any of the 10 mammary glands where tumor growth was found and digested to isolate mammary epithelial cancer cells. Total tumor weight of *Adamts1+/+* (n=10), *Adamts1+/-* (n=13) and *Adamts1-/-* (n=15) mammary tumors in proportion to body weight. b, c, d) Brightfield images of *Adamts1+/+*,

Adamts1+/- and *Adamts1-/-* 1°mMCC, revived from liquid nitrogen and grown under in vitro cell culture conditions. e, f, g) 1°mMCC immunocytostained against epithelial cell marker, cytokeratin endo-A. Images were taken at 20x magnification. h) Proportion of mammary epithelial cancer cells isolated from PyMT/*Adamts1+/+*, *Adamts1+/-* and *Adamts1-/-* mammary. Data is represented as mean ±SEM. Statistical analysis was performed using log transformed data and One-way ANOVA with Fisher's LSD post hoc test. Significance was determined if p≤0.05 (*p≤0.05, ***p≤0.0005).

expressing cells were progressively more pronounced at 1.5 h (*p*=0.005, One-way ANOVA) and 2 h (*p*=0.003, One-way ANOVA) (Fig. 4b). The rate of adhesion was determined using the slope of the regression line fitted between points from 0-2 h (*Adamts1+/+* (R^2=0.992, *p*=<0.0001); *Adamts1+/-* (R^2=0.977, *p*=<0.0001); *Adamts1-/-* (R^2=0.9370, p=<0.0001)). Consistent with the reduced adhesion index at progressive fixed time points over the course of the adhesion experiments PyMT/*Adamts-/-* cells exhibited a slower rate of adhesion to matrigel compared *Adamts1+/+* and *Adamts1+/-* cells (*p*=0.0056, One-way ANOVA, Fig. 4c).

Loss of Adamts1 impedes mammary carcinoma cell migration but had no effect on cell invasion

To investigate whether loss of *Adamts1* in mouse mammary carcinoma cells affected cancer cell motility, transwell migration assays were performed using 1°mMCC isolated from PyMT/*Adamts1+/+*, *Adamts1+/-* and *Adamts1-/-* transgenic mice (Fig. 5a). MCF10A breast epithelial cells were also included in each experiment as an inter-assay quality control of assay reproducibility and indicated a high degree of consistency between all migration assays and showed that all the primary carcinoma cells had higher migration rates than the MCF10A breast epithelial cell line (Fig. 5a, grey plot). Migratory profiles of all 1°mMCC displayed an initial phase of increasing migration index that peaked at various times for each Adamts1 genotype and plateaued thereafter (Fig. 5a). Peak migration was reached when cells saturate the underlying electrode surface, preventing further increase in cell impedance detection.

Sigmoid regression analysis was performed to objectively identify the time and maximum cell index corresponding to peak migration and the rate of migration indicated by the slope of the regression curve during active cell migration. This model fitted the profiles of each 1°mMCC almost perfectly with R^2 coefficients close to 1 (*Adamts1+/+* (R^2=0.990, *p*<0.0001),

Cellular Physiology and Biochemistry

Cell Physiol Biochem 2019;52:1553-1568

DOI: 10.33594/000000108
Published online: 29 May 2019

© 2019 The Author(s). Published by
Cell Physiol Biochem Press GmbH&Co. KG

1561

Tan et al.: Adamts1 Promotes Adhesion to ECM

Adamts1+/- (R^2=0.987, *p*<0.0001), *Adamts1-/-* (R^2=0.991, *p*<0.0001)). All primary cell lines reached similar maximum cell indices (Fig. 5c), though PyMT/*Adamts1-/-* (7.78 h ± 0.086) and *Adamts1+/-* (7.48 h ± 0.60) took longer to reach maximum migration than *Adamts+/+* mammary carcinoma cells (5.13 h ± 0.251) (*p*=0.05, One-way ANOVA; Fig. 5e). The rate of migration determined by the slope of the sigmoidal curve also depicted slower migration rates in PyMT/*Adamts1+/-* (0.3124 cell index/h ± 0.042) and PyMT/*Adamts1-/-* (0.3012 cell index/h ± 0.053) compared to wild type cells (0.562 cell index/h ±0.132) (Fig. 5g). Although the latter finding did not reach statistical significance (*p*=0.15, One-way ANOVA), the corresponding differences in migration rate and time to reach maximum migration index in PyMT/*Adamts1+/-* and PyMT/*Adamts1-/-* against PyMT/*Adamts1+/+* 1°mMCC implied that the partial or complete loss of Adamts1 expression reduced the migratory capacity of mammary carcinoma cells. Invasion of the primary cancer cells through a

Fig. 4. Loss of *Adamts1* impairs cell adhesion. a) Adhesion cell index profiles of MCF10A (n=6) Adamts1+/+ (n=8), Adamts1+/- (n=7) and Adamts1-/- (n=9) 1° mMCC over 2 h. b) Comparison of adhesion cell index of PyMT/*Adamts1+/+*, *Adamts1+/-* and *Adamts1-/-* 1°mMCC at 0.5, 1, 1.5 and 2 h c) Rate of cell adhesion over 2 h as determined by slope of the line of the linear regression model.

Matrigel barrier was assessed over 40 h. Fig. 5b presents the average invasion profiles for PyMT/*Adamts1+/+*, *Adamts1+/-* and *Adamts1-/-* cells and MCF10A. MCF10A was again used an inter-assay experimental control and revealed a high level of experimental consistency and again the MCF10A epithelial cells showed lower invasive capacity than all primary carcinoma cell lines (Fig. 5b, grey plot). No significant differences in invasion cell index were found between the three *Adamts1* 1°MCC at any time points recorded (Fig. 5b). The 40 h invasion profile was interpolated with a sigmoid regression curve to identify the time and cell index corresponding to peak invasion, and the rate of invasion. This model represented cell invasion of each sample over 40 h to a high degree (*Adamts1+/+* (R^2=0.997, p<0.0001), *Adamts1+/-* (R^2=0.990, p<0.0001), *Adamts1-/-* (R^2=0.994, p<0.0001)). Although it did not reach statistical significance, PyMT/*Adamts1-/-* 1°mMCC (1.983 ± 0.226) reached a relatively lower maximum invasion index than wild type counterparts (2.762 ± 0.05) (Fig. 5d). The total

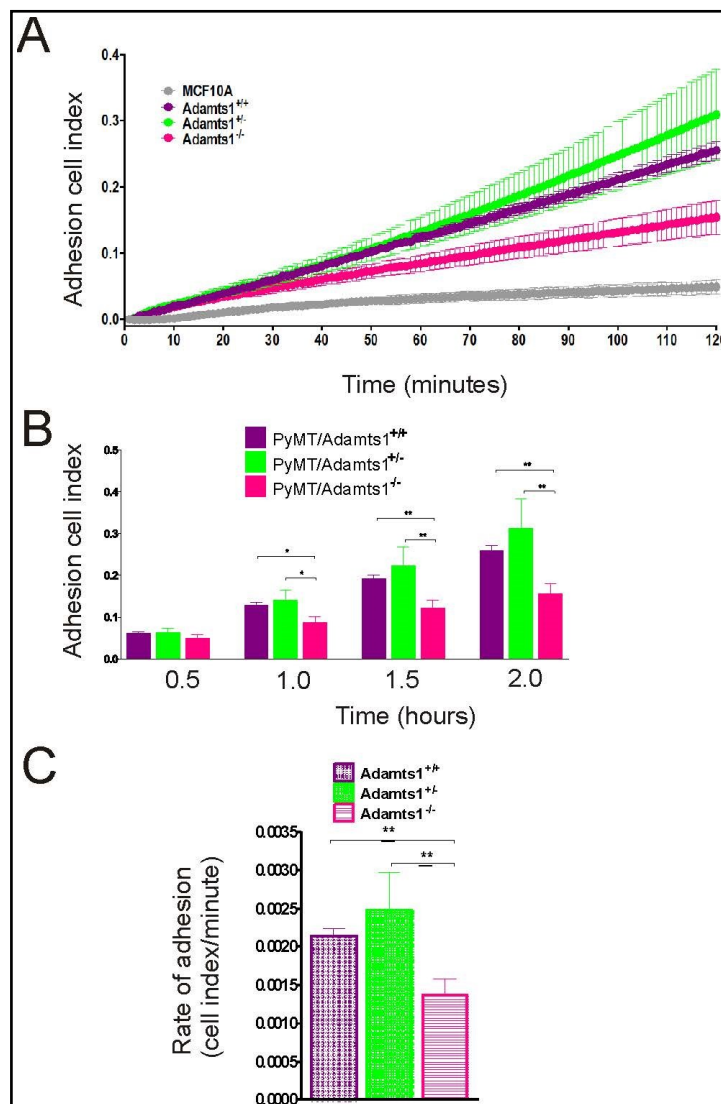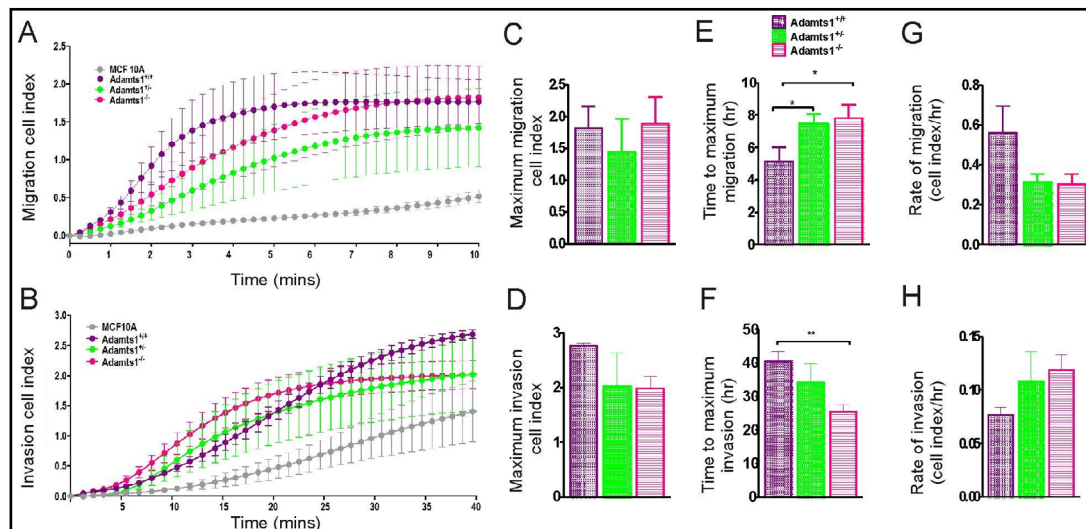**Cellular Physiology and Biochemistry**

Cell Physiol Biochem 2019;52:1553-1568

DOI: 10.33594/000000108
Published online: 29 May 2019

© 2019 The Author(s). Published by
Cell Physiol Biochem Press GmbH&Co. KG

1562

Tan et al.: Adamts1 Promotes Adhesion to ECM

Fig. 5. Loss of Adamts1 impairs cell migration but not invasion. a) Migration profiles of MCF10A (n=6) and 1°mMCC isolated from PyMT/*Adamts1+/+* (n=5), *Adamts1+/-* (n=4) and *Adamts1-/-* (n=6) mice over 10 h. b) Invasion profiles of MCF10A (n=7) and 1°mMCC isolated from *Adamts1+/+* (n=5), *Adamts1+/-* (n=5) and *Adamts1-/-*/PyMT (n=8) mice over 40 h. c, d) maximum cell index, e, f) time at which the maximum was reached and g, h) rate were determined using the sigmoid regression model. The MCF10A cell line (grey circle) was included in all assay as an inter-assay control to assess the consistency of the method. Data is represented as mean ±SEM. Statistical analysis was performed using log-transformed data and One-way ANOVA with Fisher's LSD post hoc test. Significance was determined if p≤0.05 (*p≤0.05, **p≤0.005, ≤0.0005).

time taken for maximum invasion index to be reached was significantly shorter in the PyMT/*Adamts1-/-* (25.6 h ± 2.14) cells than in the PyMT/*Adamts1+/+* 1°mMCC (40.6 h ± 2.84) (p=0.0064, One-way ANOVA with Fisher's LSD hoc test; Fig. 5f). The rate of invasion was correspondingly increased in *Adamts1+/-* and *Adamts1-/-* cells compared to *Adamts1+/+*, though this was not significant (Fig. 5h).

Discussion

MMTV-PyMT transgenic mice develop breast cancers that metastasise with high frequency, making them an important model for investigating mechanisms of metastatic progression [20]. Ablation of the *Adamts1* gene significantly reduced primary breast tumor growth in these mice and more importantly, the fatal spread of metastases to the lungs [9]. These findings demonstrated a key pro-metastatic role for ADAMTS1 in breast cancer, but how ADAMTS1 bestows pro-metastatic cell behaviour/s to mammary cancer cells is unknown. Here we showed that breast cancers in human patients also have a positive correlation between high ADAMTS1 protein abundance and increased potential to form distant metastases. Through assessment of cell-matrix adhesion, motility and invasion of primary mammary cancer cells deficient in *Adamts1*, this study found diminished capacity of PyMT/*Adamts1-/-* cells to adhere to matrigel and migrate towards a chemoattractive environment. Cell-matrix adhesion is a major cue for the determination of front-rear polarity necessary in cell migration and hence, the influence of ADAMTS1 on cell-matrix adhesion underpin its effects on breast cancer cell migration and metastasis.

Our findings of reduced ADAMTS1 protein abundance in tumours compared to normal breast tissue concurs with the many cancer studies that have also found diminished *ADAMTS1* expression in cancer tissues compared to normal tissue reviewed in [21, 22] and hence supports the proposition that ADAMTS1 may have a tumour suppressor action.

Cellular Physiology and Biochemistry

Cell Physiol Biochem 2019;52:1553-1568

DOI: 10.33594/000000108
Published online: 29 May 2019

© 2019 The Author(s). Published by
Cell Physiol Biochem Press GmbH&Co. KG

1563

Tan et al.: Adamts1 Promotes Adhesion to ECM

However, there is also strong evidence that in established malignancies, progression towards metastatic disease is associated with increased ADAMTS1 [9-11, 15, 23]. Consistent with these studies we showed that high ADAMTS1 immunostaining was associated with a higher number of positive lymph nodes and the presence of distant metastasis. Furthermore, high *ADAMTS1* was associated with reduced DFS, DMFS and OS in patients with node negative breast cancer. Together these findings suggest that elevated ADAMTS1 may confer changes in cancer cell properties and behavior that aids metastatic spread.

Dynamically changing adhesion of cells to the ECM is a key determinant of all stages of metastasis [3, 6-8, 24-26] leading us to ask whether there is an influence of Adamts1 on mammary cancer cell adhesion to the ECM. To determine whether Adamts1 elicits a change in adhesive capacity in mammary cancer cells, a series of primary cell isolates were established from *Adamts1+/+*, *Adamts1+/-* and *Adamts1-/-* PyMT mammary tumors and their capacity to adhere to matrigel was analysed. Matrigel is a heterogeneous mix of laminin, collagen IV, heparin sulphate proteoglycan, entactin and nidogen [27]. These proteins are the major constituents of the ECM and particularly basement membranes *in vivo* [26] and thus, matrigel is a widely accepted biological analogue of the extracellular environment and basement membrane *in vitro*. Finding from this study demonstrated impaired adherence of *Adamts1-/-* mouse mammary carcinoma cells to matrigel. This is a novel characteristic, which has not yet been associated with Adamts1 in breast cancer and is an important cell behaviour that could underlie the greater ability to remodel and escape the mammary duct structure and greater metastatic capacity associated with *Adamts1+/+* compared to *Adamts1* deficient mammary tumors.

Cell-ECM interactions are mediated mainly by the integrin adhesion receptors. Binding of cell surface-bound integrin receptors with protein ligands in the extracellular milieu, transduces a signalling cascade that alters focal adhesion formation as well as actin polymerisation via GTPase proteins normally activated in migrating metastatic cells [28-32]. Classical, ligand partners for integrins have been defined by the presence of an RGD (Arginine-Glycine-Asparagine) tripeptide recognition motif [33], which is not present in ADAMTS1. Over the years however, new integrin recognition sites have and are continuing to emerge [34-36] and ligand partners have diversified from ECM structural proteins, to other adhesion molecules, reviewed in [37, 38]. As a protease with a cysteine-rich disintegrin-like domain and thrombospondin motifs, Adamts1 may associate with integrins through a non-RGD motif in its disintegrin [39] and/or thrombospondin domains [25]. Indeed, a novel integrin recognition site, ECD (Glutamic acid-Cysteine-Aspartic acid), present in the ADAM metalloprotease family [40] is also present in the first thrombospondin motif of Adamts1. This tripeptide region is known to interact with αvβ3 [41], αvβ5 [42] and α6β1 [43] integrin receptors and poses as a non-RGD binding motif to which integrins such as αvβ3, αvβ5 and α6β1 can recognise and bind to. Importantly, our study addresses the complete ablation of all ADAMTS1 isoforms. At least three protein isoforms have been reported, including a 65kDa protein that does not associate with ECM, and the combination of these different forms in the tumour environment may be a determinant of the relative pro- or anti-metastatic activity. The cellular source of ADAMTS1, whether from the cancer cells themselves, or cancer associated stroma is one identified cause of different roles of ADAMTS1 in metastatic potential [44]. Here, the effect of autologous expression by the carcinoma cells on adhesion to ECM was investigated. Verification of this interaction through protein binding assessment, and whether it may influence cell-ECM adhesion has not yet been performed and is warranted in future studies.

Alternatively, Adamts1 may enhance mammary cancer cell adhesion to the ECM, through the upregulation of integrin receptors; a role which has been postulated for ADAMTS12 in human trophoblastic cells [45]. In this context and through an unknown mechanism, ADAMTS12 induced αvβ3 and αv integrins in trophoblasts, enhancing their binding to collagen II and collagen IV [45]. This reported activity attributable to ADAMTS12 proposes a mechanistic alternative with which ECM secreted enzymes such as ADAMTS1, may mediate to promote cell adherence with the ECM.

The ability to promote breast cancer cell adhesion and migration is consistent with our observed role for ADAMTS1 mammary tumour growth, progression and metastatic spread [9]. Matrix adhesion is a major cue for the acquisition of front-rear cell polarity, which dictates the opposing formation of cell-ECM contacts at the leading edge and the dissociation of cell-ECM contacts at the trailing edge [3, 4]. The unidirectional formation of focal ECM contacts and a corresponding build up of actin-cytoskeletal structure at the cell's leading edge, generate protrusion [46-48] and actomyosin contractile forces [49] that together, mechanically propel a cell forward. In enhancing the capacity of breast cancer cells to adhere to the extracellular matrix Adamts1 may promote tissue remodelling events that lead to tumor progression and spread. A study in migrating osteosarcoma cells supports this notion with localised abundance of ADAMTS1 found at the leading edge protrusion interfacing migrating cells and the adjacent matrix [50]. A similar localisation of ADAMTS1 orthologue, GON-1, was also reported in nematode Caenorhabditis elegans (*C. elegans*). In this organism, gonadal morphogenesis, which required the elongation of gonadal structures is initiated by the migration of specialised cells known as leader cells [51]. During active gonadogenesis, GON-1 expression was found specifically at the tip of the leading edge of motile leader cells [51]. Although cell adherence was not assessed in these studies, the locality of ADAMTS1 at the leading edge corresponded to the specific site where matrix contacts form.

Changes in migration could reasonably be expected to correspondingly underpin changes in invasion; however, invasion through matrigel was if anything more rapid after ablation of *Adamts1*. As PyMT/*Adamts1-/-* retain the capacity to invade, it further suggests an alternative mechanism for cell invasion that may be independent of Adamts1 proteolytic activity. It has been noted in other studies that cells can switch invasive modality, between utilising either ECM remodelling or adopt an "amoeboid" invasion mechanism [20, 25, 52-54]. Perhaps this occurs in this model of matrigel invasion by mammary carcinoma cell lines when their adhesion and migratory capacities are reduced through *Adamts1* ablation. Amoeboid cell invasion through the extracellular environment occurs independent of metalloproteolytic enzymes [41, 55-57] and is not governed by cell-matrix interactions and integrin-driven migration [20, 25, 58]. Studies have found that depletion of metalloprotease activity in cancer cells [59] including breast carcinoma cells [25] instigate the acquisition of amoeboid-like invasive phenotype as a compensatory mechanism to infiltrate the ECM. While the adhesion and migration capability of breast carcinoma cells was reduced by Adamts1 depletion, perhaps loss of ADAMTS1, instead of hindering cell invasion, altered the mode of invasion to an amoeboid, protease-independent one. Considering that the ADAMTS1 deficient tumors *in vivo* had reduced growth and metastatic properties it can be concluded that the invasive capacity of ADAMTS1 deficient cells is less aggressive and less able to establish distant metastases.

Conclusion

In conclusion, we have found that high ADAMTS1 protein abundance is associated with increased metastatic potential in human breast cancer cohorts, consistent with previous reports and our findings in the MMTV-PyMT;Adamts1-/- mouse model [9, 21]. Further, using cells derived from the mouse model our study elucidated the role for ADAMTS1 in enhancing mammary cancer cell adhesion to basement membrane-like ECM and increased capacity of mammary carcinoma cells to migrate. The capacity of breast carcinoma cells to invade, seemed unaffected by ADAMTS1 depletion. Overall, our results suggest that ADAMTS1 in malignant cells promotes metastasis by enhancing matrix adhesion and increasing motility, thereby enhancing the metastatic capacity, and consequent disease progression.

Cellular Physiology and Biochemistry

Cell Physiol Biochem 2019;52:1553-1568

DOI: 10.33594/000000108
Published online: 29 May 2019

© 2019 The Author(s). Published by
Cell Physiol Biochem Press GmbH&Co. KG

1565

Tan et al.: Adamts1 Promotes Adhesion to ECM

Acknowledgements

Disclosure Statement

The authors declare that they have no competing interests

References

1   Melzer C, von der Ohe J, Hass R: Breast Carcinoma: From Initial Tumor Cell Detachment to Settlement at Secondary Sites. Biomed Res Int 2017;2017:8534371.

2   Cao Y, Chang H, Li L, Cheng RC, Fan XN: Alteration of adhesion molecule expression and cellular polarity in hepatocellular carcinoma. Histopathology 2007;51:528-538.

3   Yamana N, Arakawa Y, Nishino T, Kurokawa K, Tanji M, Itoh R, Monypenny J, Ishizaki T, Bito H, Nozaki K, Hashimoto N, Matsuda M, Narumiya S: The Rho-mDia1 pathway regulates cell polarity and focal adhesion turnover in migrating cells through mobilizing Apc and c-Src. Mol Cell Biol 2006;26:6844-6858.

4   Muthuswamy S, Xue B: Cell polarity as a regulator of cancer cell behavior plasticity. Annu Rev Cell Dev Biol 2012;28:599-625.

5   Mi Z, Oliver T, Guo H, Gao C, Kuo P: Thrombin-cleaved COOH(-) terminal osteopontin peptide binds with cyclophilin C to CD147 in murine breast cancer cells. Cancer Res 2007;67:4088-4097.

6   Kirmse R, Otto H, Ludwig T: Interdependency of cell adhesion, force generation and extracellular proteolysis in matrix remodeling. J Cell Sci 2011;124:1857-1866.

7   Haberern C, Kupchik H: Diversity of adhesion to basement membrane components of human pancreatic adenocarcinomas. Cancer Res 1985;45:5246-5251.

8   Kramer R, McDonald K, Crowley E, Ramos D, Damsky C: Melanoma cell adhesion to basement membrane mediated by integrin-related complexes. Cancer Res 1989;49:393-402.

9   Ricciardelli C, Frewin KM, Tan Ide A, Williams ED, Opeskin K, Pritchard MA, Ingman WV, Russell DL: The ADAMTS1 protease gene is required for mammary tumor growth and metastasis. Am J Pathol 2011;179:3075-3085.

10 Kang Y, Siegel P, Shu W, Drobnjak M, Kakonen S, Cordón-Cardo C, Guise T, Massagué J: A multigenic program mediating breast cancer metastasis to bone. Cancer Cell 2003;3:537-549.

11 Minn AJ, Kang Y, Serganova I, Gupta GP, Giri DD, Doubrovin M, Ponomarev V, Gerald WL, Blasberg R, Massague J: Distinct organ specific metastatic potential of individual breast cancer cells and primary tumors. J Clin Invest 2005;115:44-55.

12 Liu YJ, Xu Y, Yu Q: Full-length ADAMTS-1 and the ADAMTS-1 fragments display pro- and antimetastatic activity, respectively. Oncogene 2006;25:2452-2467.

13 Kuno K, Bannai K, Hakozaki M, Matsushima K, Hirose K: The carboxyl-terminal half region of ADAMTS-1 suppresses both tumorigenicity and experimental tumor metastatic potential. Biochem Biophys Res Commun 2004;319:1327-1333.

14 Lu X, Wang Q, Hu G, Van Poznak C, Fleisher M, Reiss M, Massague J, Kang Y: ADAMTS1 and MMP1 proteolytically engage EGF-like ligands in an osteolytic signaling cascade for bone metastasis. Genes Dev 2009;23:1882-1894.

15 Casimiro S, Luis I, Fernandes A, Pires R, Pinto A, Gouveia AG, Francisco AF, Portela J, Correia L, Costa L: Analysis of a bone metastasis gene expression signature in patients with bone metastasis from solid tumors. Clin Exp Metastasis 2012;29:155-164.

16 Bonuccelli G, Casimiro MC, Sotgia F, Wang C, Liu M, Katiyar S, Zhou J, Dew E, Capozza F, Daumer KM, Minetti C, Milliman JN, Alpy F, Rio MC, Tomasetto C, Mercier I, Flomenberg N, Frank PG, Pestell RG, Lisanti MP: Caveolin-1 (P132L), a common breast cancer mutation, confers mammary cell invasiveness and defines a novel stem cell/metastasis-associated gene signature. Am J Pathol 2009;174:1650-1662.

17 Gyorffy B, Lanczky A, Eklund AC, Denkert C, Budczies J, Li Q, Szallasi Z An online survival analysis tool to rapidly assess the effect of 22, 277 genes on breast cancer prognosis using microarray data of 1, 809 patients. Breast Cancer Res Treat 2010;123:725-731.

18 Yung Y, Maman E, Konopnicki S, Cohen B, Brengauz M, Lojkin I, Dal Canto M, Fadini R, Dor J, Hourvitz A: ADAMTS-1: a new human ovulatory gene and a cumulus marker for fertilization capacity. Mol Cell Endocrinol 2010;328:104-108.

19 Almholt K, Juncker-Jensen A, Laerum OD, Dano K, Johnsen M, Lund LR, Romer J: Metastasis is strongly reduced by the matrix metalloproteinase inhibitor Galardin in the MMTV-PymT transgenic breast cancer model. Mol Cancer Ther 2008;7:2758-2767.

20 Sahai E, Marshall C: Differing modes of tumour cell invasion have distinct requirements for Rho/ROCK signalling and extracellular proteolysis. Nat Cell Biol 2003;5:711-719.

21 Tan Ide A, Ricciardelli C, Russell DL: The metalloproteinase ADAMTS1: a comprehensive review of its role in tumorigenic and metastatic pathways. Int J Cancer 2013;133:2263-2276.

22 Freitas VM, do Amaral JB, Silva TA, Santos ES, Mangone FR, Pinheiro Jde J, Jaeger RG, Nagai MA, Machado-Santelli GM: Decreased expression of ADAMTS-1 in human breast tumors stimulates migration and invasion. Mol Cancer 2013;12:2.

23 Masui T, Hosotani R, Tsuji S, Miyamoto Y, Yasuda S, Ida J, Nakajima S, Kawaguchi M, Kobayashi H, Koizumi M, Toyoda E, Tulachan S, Arii S, Doi R, Imamura M: Expression of METH-1 and METH-2 in pancreatic cancer. Clin Cancer Res 2001;7:3437-3443.

24 Schneider D, Liaw L, Daniel C, Athanasopoulos A, Herrmann M, Preissner K, Nawroth P, Chavakis T: Inhibition of breast cancer cell adhesion and bone metastasis by the extracellular adherence protein of Staphylococcus aureus. Biochem Biophys Res Commun 2007;357:282-288.

25 Wolf K, Mazo I, Leung H, Engelke K, von Andrian U, Deryugina E, Strongin A, Bröcker E-B, Friedl P: Compensation mechanism in tumor cell migration: mesenchymal-amoeboid transition after blocking of pericellular proteolysis. J Cell Biol 2003;160:267-277.

26 Palecek S, Loftus J, Ginsberg M, Lauffenburger D, Horwitz A: Integrin-ligand binding properties govern cell migration speed through cell-substratum adhesiveness. Nature 1997;385:537-540.

27 Kleinman H, McGarvey M, Hassell J, Star V, Cannon F, Laurie G, Martin G: Basement membrane complexes with biological activity. Biochemistry 1986;25:312-318.

28 Clark E, King W, Brugge J, Symons M, Hynes R: Integrin-mediated signals regulated by members of the rho family of GTPases. J Cell Biol 1998;142:573-586.

29 Hotchin N, Hall A: The assembly of integrin adhesion complexes requires both extracellular matrix and intracellular rho/rac GTPases. J Cell Biol 1995;131:1857-1865.

30 Ren X, Kiosses W, Schwartz M: Regulation of the small GTP-binding protein Rho by cell adhesion and the cytoskeleton. EMBO J 1999;18:578-585.

Cellular Physiology and Biochemistry

Cell Physiol Biochem 2019;52:1553-1568

DOI: 10.33594/000000108
Published online: 29 May 2019

© 2019 The Author(s). Published by
Cell Physiol Biochem Press GmbH&Co. KG

1567

Tan et al.: Adamts1 Promotes Adhesion to ECM

31   Ridley A, Hall A: The small GTP-binding protein rho regulates the assembly of focal adhesions and actin stress fibers in response to growth factors. Cell 1992;70:389-399.

32   Price L, Leng J, Schwartz M, Bokoch G: Activation of Rac and Cdc42 by integrins mediates cell spreading. Mol Biol Cell 1998;9:1863-1871.

33   Pierschbacher M, Ruoslahti E: Variants of the cell recognition site of fibronectin that retain attachment-promoting activity. Proc Natl Acad Sci U S A 1984;81:5985-5988.

34   McCarthy J, Skubitz A, Qi Z, Yi X, Mickelson D, Klein D, Furcht L: RGD-independent cell adhesion to the carboxy-terminal heparin-binding fragment of fibronectin involves heparin-dependent and -independent activities. J Cell Biol 1990;110:777-787.

35   Humphries M, Yasuda Y, Olden K, Yamada K: The cell interaction sites of fibronectin in tumour metastasis. Ciba Found Symp 1988;141:75-93.

36   Soteriadou K, Remoundos M, Katsikas M, Tzinia A, Tsikaris V, Sakarellos C, Tzartos S: The SerArg-Tyr-Asp region of the major surface glycoprotein of Leishmania mimics the Arg-Gly-Asp-Ser cell attachment region of fibronectin. J Biol Chem 1992;267:13980-13985.

37   Humphries J, Byron A, Humphries M: Integrin ligands at a glance. J Cell Sci 2006;119:3901-3903.

38   Plow E, Haas T, Zhang L, Loftus J, Smith J: Ligand binding to integrins. J Biol Chem 2000;275:21785-21788.

39   McLane M, Sanchez E, Wong A, Paquette-Straub C, Perez J: Disintegrins. Curr Drug Targets Cardiovasc Haematol Disord 2004;4:327-355.

40   Kirmse R, Otto H, Ludwig T: Interdependency of cell adhesion, force generation and extracellular proteolysis in matrix remodeling. J Cell Sci 2011;124:1857-1866.

41   Yokotsuka M, Iwaya K, Saito T, Pandiella A, Tsuboi R, Kohno N, Matsubara O, Mukai K: Overexpression of HER2 signaling to WAVE2-Arp2/3 complex activates MMP-independent migration in breast cancer. Breast Cancer Res Treat 2011;126:311-318.

42   Yu X, Machesky L: Cells assemble invadopodia-like structures and invade into matrigel in a matrix metalloprotease dependent manner in the circular invasion assay. PloS One 2012;7:e30605.

43   Tester A, Ruangpanit N, Anderson R, Thompson E: MMP-9 secretion and MMP-2 activation distinguish invasive and metastatic sublines of a mouse mammary carcinoma system showing epithelial-mesenchymal transition traits. Clin Exp Metastasis 2000;18:553-560.

44   Fernandez-Rodriguez R, Rodriguez-Baena FJ, Martino-Echarri E, Peris-Torres C, Del Carmen Plaza-Calonge M, Rodriguez-Manzaneque JC: Stroma-derived but not tumor ADAMTS1 is a main driver of tumor growth and metastasis. Oncotarget 2016;7:34507-34519.

45   Beristain AG, Zhu H, Leung PC: Regulated expression of ADAMTS-12 in human trophoblastic cells: a role for ADAMTS-12 in epithelial cell invasion? PLoS One 2011;6:e18473.

46   Bugyi B, Carlier MF: Control of actin filament treadmilling in cell motility. Annu Rev Biophys 2010;39:449-470.

47   Le Clainche C, Carlier MF. Actin-based motility assay. Curr Protoc Cell Biol 2004; DOI:10.1002/0471143030.cb1207s24.

48   Pollard T, Borisy G: Cellular motility driven by assembly and disassembly of actin filaments. Cell 2003;112:453-465.

49   Iwadate Y, Yumura S: Actin-based propulsive forces and myosin-II-based contractile forces in migrating Dictyostelium cells. J Cell Sci 2008;121:1314-1324.

50   Rehn A, Birch M, Karlström E, Wendel M, Lind T: ADAMTS-1 increases the three dimensional growth of osteoblasts through type I collagen processing. Bone 2007;41:231-238.

51   Blelloch R, Kimble J: Control of organ shape by a secreted metalloprotease in the nematode Caenorhabditis elegans. Nature 1999;399:586-590.

52   Rösel D, Brábek J, Tolde O, Mierke C, Zitterbart D, Raupach C, Bicanová K, Kollmannsberger P, Panková D, Vesely P, Folk P, Fabry B: Up-regulation of Rho/ROCK signaling in sarcoma cells drives invasion and increased generation of protrusive forces. Mol Cancer Res 2008;6:1410-1420.

53   Sabeh F, Shimizu-Hirota R, Weiss S: Protease-dependent versus -independent cancer cell invasion programs: three-dimensional amoeboid movement revisited. J Cell Biol 2009;185:11-19.

54   Farina K, Wyckoff J, Rivera J, Lee H, Segall J, Condeelis J, Jones J: Cell motility of tumor cells visualized in living intact primary tumors using green fluorescent protein. Cancer Res 1998;58:2528-2532.

55 Guiet R, Van Goethem E, Cougoule C, Balor S, Valette A, Al Saati T, Lowell C, Le Cabec V, Maridonneau-Parini I: The process of macrophage migration promotes matrix metalloproteinase-independent invasion by tumor cells. J Immunol 2011;187:3806-3814.

56 Grise F, Sena S, Bidaud-Meynard A, Baud J, Hiriart J-B, Makki K, Dugot-Senant N, Staedel C, Bioulac-Sage P, Zucman-Rossi J, Rosenbaum J, Moreau V: Rnd3/RhoE Is downregulated in hepatocellular carcinoma and controls cellular invasion. Hepatology 2012;55:1766-1775.

57 Hancox R, Allen M, Holliday D, Edwards D, Pennington C, Guttery D, Shaw J, Walker R, Pringle J, Jones J: Tumour associated tenascin-C isoforms promote breast cancer cell invasion and growth by matrix metalloproteinase-dependent and independent mechanisms. Breast Cancer Res 2009;11:R24.

58 Terry S, Elbediwy A, Zihni C, Harris A, Bailly M, Charras G, Balda M, Matter K: Stimulation of cortical myosin phosphorylation by p114rhogef drives cell migration and tumor cell invasion. PloS One 2012;7:e50188.

59 Meierjohann S, Hufnagel A, Wende E, Kleinschmidt M, Wolf K, Friedl P, Gaubatz S, Schartl M: MMP13 mediates cell cycle progression in melanocytes and melanoma cells: *in vitro* studies of migration and proliferation. Mol Cancer 2010;9:201.